This is the author's version of an article that has been published in this journal. Changes were made to this version by the publisher prior to publication. The final version is available at http://dx.doi.org/10.1109/LMWT.2025.3560909

Cognitive Broyden-based Input Space Mapping for Design Optimization

José E. Rayas-Sánchez

***Abstract*—Cognition-driven design of RF and microwave circuits is an emerging and promising approach to efficient design optimization of computationally expensive fine models. Existing techniques for cognition-driven design have been developed for optimizing microwave filters without exploiting traditional coarse model representations, e.g., equivalent circuits. Instead, intermediate feature-space parameters have been used to establish other types of mappings in the design process. In this paper, a cognitive space mapping (SM) technique that fully exploits traditional coarse models is proposed for the first time. The proposed cognitive SM approach exploits a previous cognition-driven parameter extraction (PE) formulation at each SM iteration. This cognitive SM technique follows an algorithmic structure that is an extension of that one used by the Broyden-based input SM, better known as aggressive space mapping (ASM). A synthetic benchmark example illustrates the performance improvement of the proposed cognitive SM versus ASM.**

***Index Terms*—Broyden, Chebyshev, cognition, Euclidean, Kullback-Leibler, Manhattan, norm, objective function, optimization, parameter extraction, space mapping.**

I. Introduction

In the arena of computer-aided design (CAD) and electronic design automation (EDA), the concept of cognition-driven design can be characterized as the systematic incorporation of key engineering knowledge, experience, and human intuition, in automated numerical algorithmic techniques to make the modeling and design optimization processes more efficient and accurate [1]. This general concept of cognition-driven design for RF and microwave circuits was first proposed by Prof. John Bandler [2], who also speculated on the exploitation of neuroscience in engineering design.

Space mapping (SM), invented by Bandler *et al.* [3], represents a great example of how the design optimization of highly accurate but computationally expensive models (known as fine models) can be dramatically accelerated by exploiting prior engineering knowledge in the form of available equivalent circuit models and other physics-based simplified representations (known as coarse models) [4], [5]. SM techniques were originally formulated to optimize full-wave EM models in microwave circuits [6], however, they were later successfully adapted to address many other engineering problems [3], [7].

Pioneering contributions to cognition-driven design of RF and microwave filters have already been developed [8]-[10]. These cognition-driven approaches address design problems where no explicit coarse model is available, and hence, no mapping can be established between the coarse and fine model traditional design spaces [3]. Instead, intermediate feature-space parameters [8], *e.g.*, feature frequency parameters and ripple height parameters, are employed to establish other types of mappings. The traditional design parameters are mapped to several (cascaded) feature parameters for efficient filter design optimization [8], [9]. Similarly, cognition-driven multiphysics optimization for microwave filters is in [11] by using feature-based neural models. Modeling and design optimization of microwave circuits based on response features have also been contributed [12]-[15], where surrogate metamodels with no SM incorporating physics-based coarse models are employed.

In contrast to the previous cognition-driven design techniques, here, a cognitive space mapping technique fully exploiting traditional coarse models is proposed for the first time. The proposed cognitive space mapping formulation builds on an initial investigation about cognition-driven parameter extraction (PE) presented in [16]. In that work, it is demonstrated that cognitive PE formulations yield more accurate extracted parameters and achieve a more meaningful matching with less variability regardless of the type of PE objective function employed, considering Manhattan, Euclidean, Chebyshev, and Kullback-Leibler (K-L) objectives [17]. The conclusions found in [16] are independent of the numerical optimization method employed for PE since they are based on graphical studies conducted over large regions of the coarse model design space. The present paper exploits [16] to propose a novel cognitive space mapping formulation whose algorithmic structure is an extension of that one employed in the classical and popular aggressive space mapping (ASM) [7]. Through the use of a synthetic benchmark example, it is illustrated how the proposed cognitive Broyden-based input SM approach can significantly enhance the performance of traditional SM.

II. Brief Description of the Cognitive Broyden-based Input Space Mapping

As in most SM optimization approaches, the proposed cognitive SM starts by applying direct optimization to the coarse model, by solving

$$\boldsymbol{x}_c^* = \arg\min_{\boldsymbol{x}_c} U\left(\boldsymbol{R}_c(\boldsymbol{x}_c)\right) \tag{1}$$

This article was presented at the IEEE MTT-S International Microwave Symposium (IMS 2025), San Francisco, CA, USA, June 15–20, 2025.

José Ernesto Rayas-Sánchez is with the Department of Electronics, Systems, and Informatics, ITESO – The Jesuit University of Guadalajara, Tlaquepaque, Jalisco, 45604 Mexico. e-mail: erayas@iteso.mx.

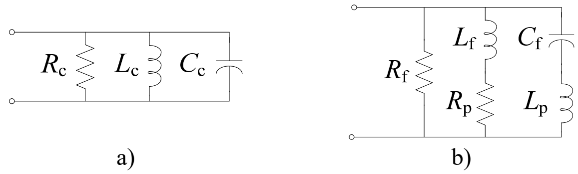

Fig. 1. Benchmark synthetic lumped resonator [19] to compare classical versus cognitive Broyden-based input space mapping optimization: (a) the coarse model is an ideal lumped RLC parallel resonator with design parameters $\boldsymbol{x}_c = [R_c(\Omega)\ \ L_c(\text{nH})\ \ C_c(\text{pF})]^T$ (b) the "fine" model has some parasitic elements R_p and L_p, and it has design parameters $\boldsymbol{x}_f = [R_f(\Omega)\ \ L_f(\text{nH})\ \ C_f(\text{pF})]^T$.

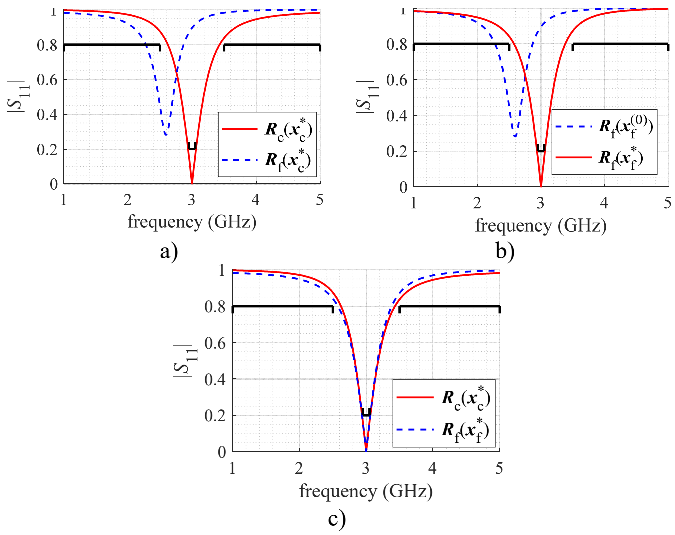

Fig. 2. Responses of the lumped resonator: a) optimal coarse model response $\boldsymbol{R}_c(\boldsymbol{x}_c^*)$ and fine model response $\boldsymbol{R}_f$ at the coarse model optimal design $\boldsymbol{x}_c^*$ (this is the starting point for SM); b) optimal fine model response, $\boldsymbol{R}_f(\boldsymbol{x}_f^*)$, where the fine model optimal design $\boldsymbol{x}_f^*$ is obtained from direct minimax optimization (see Fig. 3) using a starting point $\boldsymbol{x}_f^{(0)} = \boldsymbol{x}_c^*$; c) comparing both optimal responses.

where $\boldsymbol{R}_c(\boldsymbol{x}_c)$ represents coarse model response at a given coarse model design $\boldsymbol{x}_c$, U is a suitable objective function expressed in terms of the model responses and the design specifications, and $\boldsymbol{x}_c^*$ is the optimal coarse model design.

Next, the fine model $\boldsymbol{R}_f(\boldsymbol{x}_f)$ is evaluated at the starting point $\boldsymbol{x}_f^{(0)} = \boldsymbol{x}_c^*$. Normally, $\boldsymbol{R}_f(\boldsymbol{x}_c^*)$ either violates the design specifications or is sub-optimal.

Parameter extraction (PE) is next performed. It consists of a local alignment between the coarse and fine model responses at the current iteration i. In conventional SM approaches, PE is typically done by solving

$$\boldsymbol{x}_c^{\text{PE}} = \arg\min_{\boldsymbol{x}_c} U_{\text{PE}}\left(\boldsymbol{R}_c(\boldsymbol{x}_c), \boldsymbol{R}_f(\boldsymbol{x}_f^{(i)})\right) \tag{2}$$

where $\boldsymbol{x}_c^{\text{PE}}$ has the extracted parameters at the i-th SM iteration, $\boldsymbol{R}_f(\boldsymbol{x}_f^{(i)})$ is the current target response, and U_{PE} is a suitable objective function for PE, *e.g.*, Manhattan, Euclidean, Chebyshev, or Kullback-Leibler (K-L) [17]. After solving (2), $\boldsymbol{R}_c(\boldsymbol{x}_c^{\text{PE}}) \approx \boldsymbol{R}_f(\boldsymbol{x}_f^{(i)})$.

Following [16], instead of solving (2), a cognition-driven PE is performed by solving

$$\boldsymbol{x}_c^{\text{PE}} = \arg\min_{\boldsymbol{x}_c} U_{\text{PE}}\left(\boldsymbol{\Phi}(\boldsymbol{R}_c(\boldsymbol{x}_c)), \boldsymbol{\Phi}(\boldsymbol{R}_f(\boldsymbol{x}_f^{(i)}))\right) \tag{3}$$

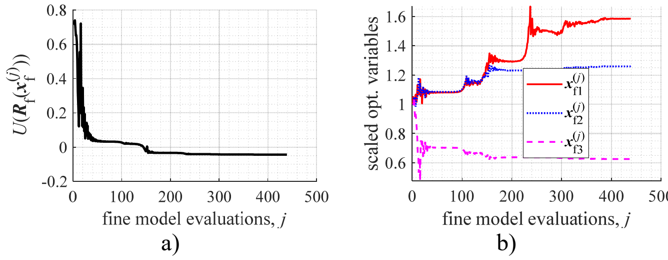

Fig. 3. Applying direct optimization to the fine model: a) evolution of the minimax objective function; b) evolution of the optimization variables.

where $\boldsymbol{\Phi}$ is a suitable encoding function that translates the traditional circuit responses (*e.g.*, S-parameters evaluated over the whole frequency sweeps) into key feature responses that are problem dependent. Engineering expertise and intuition on the problem in hand is fundamental for determining $\boldsymbol{\Phi}$.

As in any Broyden-based input SM, the next iterate $\boldsymbol{x}_f^{(i+1)} = \boldsymbol{x}_f^{(i)} + \boldsymbol{h}$ is predicted from a quasi-Newton step $\boldsymbol{h}$ by solving the linear approximation

$$\boldsymbol{B}\boldsymbol{h} = -\left(\boldsymbol{x}_c^{\text{PE}} - \boldsymbol{x}_c^*\right) \tag{4}$$

where $\boldsymbol{B}$ is the Broyden matrix that approximates the Jacobian of the corresponding system of nonlinear equations [7] at each SM iteration. After solving (4), $\boldsymbol{B}$ is updated using its classical rank-one updating formula [18], [7]. Keeping matrix $\boldsymbol{B}$ well-conditioned at all SM iterations is key to avoid oscillations or even divergence.

If the extracted parameters $\boldsymbol{x}_c^{\text{PE}}$ after solving (2) or (3) are sufficiently closed to the optimal coarse model design $\boldsymbol{x}_c^*$, then SM ends, since that implies that the current fine model response $\boldsymbol{R}_f(\boldsymbol{x}_f^{(i)})$ is close enough to the optimal coarse model response $\boldsymbol{R}_c(x_c^*)$, which plays the role of the desired response for the fine model.

III. SM Example: Synthetic Lumped Resonator

Consider a classical benchmark SM problem consisting of a synthetic lumped equivalent-circuit resonator [19]. The coarse and "fine" models are illustrated in Fig. 1. The coarse model is an ideal canonical parallel lumped resonator (see Fig. 1a), whose design parameters are $\boldsymbol{x}_c = [R_c(\Omega)\ \ L_c(\text{nH})\ \ C_c(\text{pF})]^T$. The "fine" model, whose design parameters are $\boldsymbol{x}_f = [R_f(\Omega)\ \ L_f(\text{nH})\ \ C_f(\text{pF})]^T$, consists of the same parallel lumped resonator but with some parasitic elements (see Fig. 1b): a parasitic series resistor $R_p = 0.3\ \Omega$ associated to the inductance L_f, and a parasitic series inductance $L_p = 0.09$ nH associated to the capacitor C_f. Boths models use a reference impedance $Z_0 = 50\ \Omega$.

The design specifications are:

$$|S_{11}| \geq 0.8 \text{ for } 1 \text{ GHz} \leq f \leq 2.5 \text{ GHz} \tag{5a}$$

$$|S_{11}| \leq 0.2 \text{ for } 2.95 \text{ GHz} \leq f \leq 3.05 \text{ GHz} \tag{5b}$$

$$|S_{11}| \geq 0.8 \text{ for } 3.5 \text{ GHz} \leq f \leq 5 \text{ GHz} \tag{5c}$$

The optimal coarse model design, obtained from direct minimax optimization [19], is $\boldsymbol{x}_c^* = [50\ \ 0.2683\ \ 10.4938]^T$. The corresponding optimal coarse model response, $\boldsymbol{R}_c(x_c^*)$, is shown in Fig. 2a, which satisfies the design specifications.

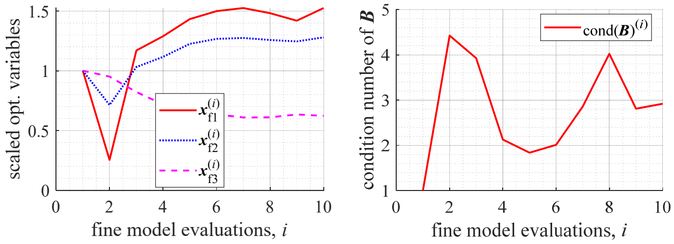

a) b)

Fig. 4. Conventional Broyden-based input SM optimization results: a) evolution of the scaled optimization variables; b) evolution of the condition number of the Broyden matrix $\boldsymbol{B}$. This technique solves the problem in only 10 fine model evaluations.

Evaluating the fine model at $\boldsymbol{x}_c^*$ yields the starting point for SM. Fig. 2a confirms that the "fine" model violates the design specifications when evaluated at $\boldsymbol{x}_c^*$.

A. Direct Optimization of the Fine Model

Since this "fine" model is computationally cheap, we can directly optimize it to get the actual fine model design $\boldsymbol{x}_f^*$ as a reference for comparison. Applying the gradient-free Nelder-Mead optimization method directly to the fine model, with a minimax formulation using the design specifications (5) and a starting point $\boldsymbol{x}_f^{(0)} = \boldsymbol{x}_c^*$, $\boldsymbol{x}_f^* = [79.2239 \quad 0.3378 \quad 6.5667]^T$ is obtained after 439 fine model evaluations. The corresponding optimal fine response $\boldsymbol{R}_f(x_f^*)$ is in Fig. 2b and compared with $\boldsymbol{R}_c(x_c^*)$ in Fig. 2c. It is seen that $\boldsymbol{R}_f(x_f^*)$ satisfies the design specifications. The evolution of the fine model minimax objective function U during direct optimization is in Fig. 3a, while the corresponding evolution of the scaled optimization variables is in Fig. 3b (scaled with respect to $\boldsymbol{x}_f^{(0)} = \boldsymbol{x}_c^*$).

B. Applying Conventional Space Mapping

The conventional Broyden-based input space mapping

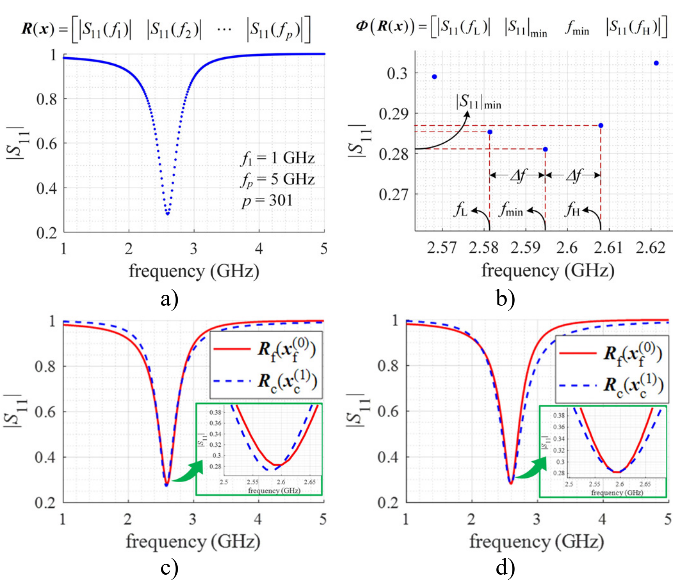

Fig. 5. First PE in SM optimization: a) conventional target response and c) corresponding matching after PE; b) cognitive target response as defined in (6) and d) corresponding matching after PE.

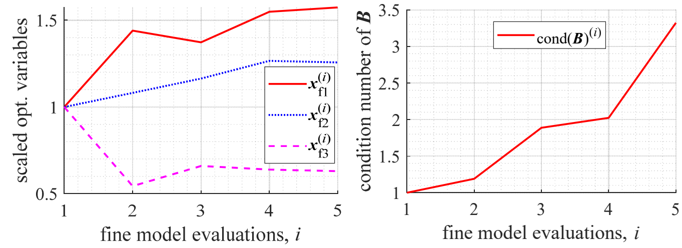

a) b)

Fig. 6. Cognitive Broyden-based input SM optimization results: a) evolution of the scaled optimization variables; b) evolution of the condition number of the Broyden matrix $\boldsymbol{B}$. This technique solves the problem in only 5 fine model evaluations.

technique (or ASM) [7] is now applied to this benchmark problem. Even though this problem looks extremely simple (see Fig. 1), it can be very challenging for SM due to the highly nonlinear mapping between the coarse and fine model design parameters [7]. As demonstrated in [19], conventional Broyden-based input SM diverges when trying to solve this problem with large parasitic element values, *e.g.*, $R_p = 0.5\ \Omega$ and $L_p = 0.13$ nH. To obtain quantifiable results for numerical comparisons, smaller parasitic values are used here ($R_p = 0.3\ \Omega$ and $L_p = 0.09$ nH).

Conventional Broyden-based input SM is able to solve this problem in just 9 SM iterations (or 10 fine model evaluations). Parameter extraction at each SM iteration is done by matching $|S_{11}|$ in the whole frequency sweep (1-5 GHz, with $p = 301$ frequency points), using a conventional Manhattan norm. The evolution of the scaled optimization variables is in Fig. 4a, which represents a huge improvement with respect to that one in Fig. 3b from direct fine model optimization, as expected. The SM solution found is $\boldsymbol{x}_f^{SM} = [76.1971 \quad 0.3432 \quad 6.5346]^T$. The corresponding evolution of the condition number of the Broyden matrix $\boldsymbol{B}$ is shown in Fig. 4b, confirming that $\boldsymbol{B}$ remains well conditioned during the whole SM optimization.

C. Applying Cognitive Space Mapping

The proposed cognition SM formulation is now applied to the same problem. Considering the typical responses that can be obtained from both (coarse and fine) resonant circuits, instead of matching $|S_{11}|$ in the full frequency band during PE at each SM iteration, a more meaningful feature response $\boldsymbol{\Phi}$ is selected for PE. Here, $\boldsymbol{\Phi}$ is selected as

$$\boldsymbol{\Phi}(\boldsymbol{R}(\boldsymbol{x})) = \left[|S_{11}(f_L)| \quad |S_{11}|_{min} \quad f_{min} \quad |S_{11}(f_H)|\right] \tag{6a}$$

where $|S_{11}|_{min}$ is the minimum value of $|S_{11}|$ in the whole frequency sweep, f_{min} is the frequency where that minimum is located, and f_L and f_H are two neighboring frequency points defined as

$$f_L = f_{min} - \Delta f \quad \text{and} \quad f_H = f_{min} + \Delta f \tag{6b}$$

where Δf is a suitable perturbation (in this case, $\Delta f = (5-1)$ GHz / $(p-1) = 13.33$ MHz, but other points around f_{min} can be selected). Fig. 5 contrasts a conventional target response versus a cognitive one for PE at the first SM iteration in this problem. It is seen that the cognitive approach using suitable

TABLE I. COMPARING FINAL SM RESULTS FOR THE LUMPED RLC RESONATOR USING CONVENTIONAL VS. COGNITIVE SM FORMULATIONS

SM formulation	N_{fme}	$\boldsymbol{x}_{\mathrm{f}}^{\mathrm{SM}}$	$\varepsilon_{\mathrm{avg}}^{\mathrm{SM}}$	$\varepsilon_{\mathrm{max}}^{\mathrm{SM}}$	$\varepsilon_{\mathrm{nms}}^{\mathrm{SM}}$
Conventional	10	$[76.1971\ \ 0.3432\ \ 6.5346]^{\mathrm{T}}$	1.2893	3.8206	3.8077
Cognitive	5	$[78.7016\ \ 0.3373\ \ 6.6110]^{\mathrm{T}}$	0.2386	0.6593	0.6594

N_{fme}: total number of fine model evaluations.

feature responses $\boldsymbol{\Phi}$ for PE yields better local alignment between the two models. This also happens in subsequent SM iterations, yielding a better SM evolution. Examples on how to define suitable features for other types of responses (a lowpass filter and an impedance matching network) are found in [16].

By using this more intelligently adapted response $\boldsymbol{\Phi}$ to the problem in hand, significantly better SM results are obtained. The SM solution $\boldsymbol{x}_{\mathrm{f}}^{\mathrm{SM}} = [78.7016\ \ 0.3373\ \ 6.6110]^{\mathrm{T}}$ is found in just 4 SM iterations (5 fine model evaluations). The evolution of the scaled optimization variables is shown in Fig. 5a. The evolution of the condition number of matrix $\boldsymbol{B}$ is shown in Fig. 5b, which indicates a much better conditioned $\boldsymbol{B}$ during the whole SM optimization than conventional SM; this contributes to the better next iterates.

D. Numerical Comparison between the Two SM Formulations

In addition to the previously illustrated performance comparison between the conventional and cognitive SM formulations, in terms of the number of iterations, fine model evaluations, and condition number of the Broyden matrix, Table I summarizes a comparison in terms of the accuracy of the space-mapped solution found $\boldsymbol{x}_{\mathrm{f}}^{\mathrm{SM}}$ by each formulation.

The following error metrics are used to assess the accuracy of the SM solution $\boldsymbol{x}_{\mathrm{f}}^{\mathrm{SM}}$ with respect to the actual fine model optimal design $\boldsymbol{x}_{\mathrm{f}}^{*}$: the average absolute relative error ($\varepsilon_{\mathrm{avg}}^{\mathrm{SM}}$), the maximum absolute relative error ($\varepsilon_{\mathrm{max}}^{\mathrm{SM}}$), and the normalized mean square error ($\varepsilon_{\mathrm{nms}}^{\mathrm{SM}}$), defined as

$$\varepsilon_{\mathrm{avg}}^{\mathrm{SM}} = \frac{100}{n}\frac{\| \boldsymbol{x}_{\mathrm{f}}^{\mathrm{SM}} - \boldsymbol{x}_{\mathrm{f}}^{*} \|_1}{\| \boldsymbol{x}_{\mathrm{f}}^{*} \|_\infty}\ (\%) \tag{7a}$$

$$\varepsilon_{\mathrm{max}}^{\mathrm{SM}} = 100\frac{\| \boldsymbol{x}_{\mathrm{f}}^{\mathrm{SM}} - \boldsymbol{x}_{\mathrm{f}}^{*} \|_\infty}{\| \boldsymbol{x}_{\mathrm{f}}^{*} \|_\infty}\ (\%) \tag{7b}$$

$$\varepsilon_{\mathrm{nms}}^{\mathrm{SM}} = 100\frac{\| \boldsymbol{x}_{\mathrm{f}}^{\mathrm{SM}} - \boldsymbol{x}_{\mathrm{f}}^{*} \|_2}{\| \boldsymbol{x}_{\mathrm{f}}^{*} \|_2}\ (\%) \tag{7c}$$

It is seen from Table I that the cognitive SM formulation yields a more accurate solution with a much smaller computational cost in terms of fine model evaluations.

IV. CONCLUSION

A cognition-driven space mapping technique exploiting physics-based coarse models was presented. It employs cognitive parameter extraction and a Broyden update at each space mapping iteration. The proposed formulation is an emerging and promising approach to further increase the famous efficiency of space mapping.

REFERENCES

[1] J. E. Rayas-Sánchez, S. Koziel, and J. W. Bandler, "Advanced RF and microwave design optimization: a journey and a vision of future trends," *IEEE J. of Microwaves*, vol. 1, no. 1, pp. 481-493, Jan. 2021.

[2] J. E. Rayas-Sánchez, Q. J. Zhang, J. W. Rautio, N. K. Nikolova, V. E. Boria, Q. S. Cheng, M. Yu, and W. J. R. Hoefer, "Microwave modeling and design optimization: The legacy of John Bandler," *IEEE Trans. Microwave Theory Techn.*, vol. 73, no. 1, pp. 87-101, Jan. 2025.

[3] J. W. Bandler and J. E. Rayas-Sánchez, "An early history of optimization technology for automated design of microwave circuits," *IEEE J. of Microwaves*, vol. 3, no. 1, pp. 319-337, Jan. 2023.

[4] J. W. Bandler, Q. Cheng, S. A. Dakroury, A. S. Mohamed, M. H. Bakr, K. Madsen and J. Søndergaard, "Space mapping: the state of the art," *IEEE Trans. Microwave Theory Techn.*, vol. 52, no. 1, pp. 337-361, Jan. 2004.

[5] S. Koziel, Q. S. Cheng, and J. W. Bandler, "Space mapping," *IEEE Microwave Magazine*, vol. 9, no. 6, pp. 105-122, Dec. 2008.

[6] J. W. Bandler, R. M. Biernacki, S. H. Chen, P. A. Grobelny, and R. H. Hemmers, "Space mapping technique for electromagnetic optimization," *IEEE Trans. Microwave Theory Tech.*, vol. 42, no. 12, pp. 2536–2544, Dec. 1994.

[7] J. E. Rayas-Sánchez, "Power in simplicity with ASM: tracing the aggressive space mapping algorithm over two decades of development and engineering applications," *IEEE Microwave Magazine*, vol. 17, no. 4, pp. 64-76, Apr. 2016.

[8] C. Zhang, F. Feng, V. Gongal-Reddy, Q. J. Zhang, and J. W. Bandler, "Cognition-driven formulation of space mapping for equal-ripple optimization of microwave filters," *IEEE Trans. Microwaves Theory Techn.*, Vol. 63, no. 7, pp. 2154-2165, Jul. 2015.

[9] C. Zhang, F. Feng, Q.J. Zhang, and J.W. Bandler, "An enhanced cognition-driven formulation of space mapping for equal-ripple optimization of microwave filters," *IET Microwaves Antennas Propag.*, vol. 12, no. 1, pp. 82-91, Jan. 2018.

[10] J. Jin, F. Feng, W. Na, J. Zhang, W. Zhang, Z.H. Zhao, and Q.J. Zhang, "Advanced cognition-driven EM optimization incorporating transfer function-based feature surrogate for microwave filters," *IEEE Trans. Microwave Theory Techn.*, vol. 69, no. 1, pp. 15-28, Jan. 2021.

[11] J. Fu, J. Jin, K. Cao, T. Li, X. Shi, and H. Lin, "Two-stage cognition-driven multiphysics optimization for microwave filters design," *Photonics Electromag. Research Symp. (PIERS)*, Chengdu, China, Apr. 2024, pp. 1-5.

[12] S. Koziel, Q. S. Cheng, and J. W. Bandler, "Feature-based surrogates for low-cost microwave modelling and optimization," *IET Microw., Antennas Propag.*, vol. 9, no 15, p. 1706-1712, 2015.

[13] A. Pietrenko-Dabrowska and S. Koziel, "Generalized formulation of response features for reliable optimization of antenna input characteristics," *IEEE Trans. Antennas Propag.*, vol. 70, no. 5, pp. 3733-3748, May 2022.

[14] S. Koziel, A. Pietrenko-Dabrowska and P. Plotka, "On improved-reliability design optimization of high-frequency structures using local search algorithms," *IEEE Access*, vol. 10, pp. 90586-90596, Aug. 2022.

[15] L. Bi, W. Cao, Y. Shi, W. Hu, L. Guo, and M. Wu, "Dynamic hybrid models with active sampling and adaptive selection of double-domain features for the tuning of microwave cavity filters," *IEEE Trans. Cybernetics*, vol. 54, no. 8, pp. 4828-4840, Aug. 2024.

[16] J. E. Rayas-Sánchez, "Cognitive parameter extraction for space mapping design optimization," in *IEEE MTT-S Latin America Microwave Conf. (LAMC-2025)*, San Juan, Puerto Rico, Jan. 2025, pp. 9-12.

[17] R. Loera-Díaz and J. E. Rayas-Sánchez, "An objective function formulation for circuit parameter extraction based on the Kullback-Leibler distance," in *IEEE MTT-S Int. Microwave Symp. Dig.*, Los Angeles, CA, Jun. 2020, pp. 80-82.

[18] C. G. Broyden, "A class of methods for solving non-linear simultaneous equations", *Math. Comp.*, vol. 19, no. 92, pp. 577-593, Oct. 1965.

[19] J. E. Rayas-Sánchez, F. Lara-Rojo, and E. Martínez-Guerrero, "A linear inverse space mapping (LISM) algorithm to design linear and nonlinear RF and microwave circuits," *IEEE Trans. Microwave Theory Techn.*, vol. 53, no. 3, pp. 960-968, Mar. 2005.